Photoelectrochemical Charge Transfer Properties of Electrodeposited CdSe Quantum Dots

Boaz Alperson, Helene Demange, Israel Rubinstein, and Gary Hodes*

Department of Materials and Interfaces, The Weizmann Institute of Science, Rehovot 76100, Israel

Received: August 13, 1998; In Final Form: February 21, 1999

The blue shift in the optical band gap of CdSe quantum dot films was measured using liquid-junction photoresponse spectroscopy and correlated to nanocrystalline dimensions measured by transmission electron microscopy and X-ray diffractometry. Differences in the internal collection efficiency from films of various thicknesses are discussed in terms of both charge and energy transfer mechanisms. Pronounced sub-band-gap signals from intra-band-gap states have been observed. Features in the short wavelength region of the spectra have been attributed to charge transport involving hot holes.

Introduction

In semiconductor quantum dots (QDs), there is a gradual transition from solid state to molecular structure as the crystallite size decreases. Consequently, a change in the energy band structure occurs, expressed as an increase in the effective optical band gap (blue shift) and a change from a continuum (band) to discrete, quantized energy levels.[1] Thus, semiconductor QD films can be used for band gap tailoring, a property of particular importance for photovoltaic cells where the band gap value is a critical parameter.

In photoelectrochemical cells, the built-in space charge layer is formed by a junction between the semiconductor and an electrolyte (usually liquid). The photoelectrochemistry of nanocrystalline semiconductor films has been the subject of considerable attention recently. Such studies can be divided into sensitized nanocrystalline cells (usually using dyes), where light is absorbed in the sensitizer and charge is transferred to the nanocrystalline film,[2] and nonsensitized films, where the light is absorbed in the semiconductor itself.[3−5] In the latter, for very small nanocrystals, where little or no space charge layer is present in the individual nanocrystals, charge separation occurs as a result of the different kinetics of electron and hole transfer from the semiconductor to the electrolyte.[6,7]

We have previously described the electrodeposition of CdSe quantum dots onto (111) textured gold films.[8] The first layer of crystals was epitaxial with the gold substrate, and the nanocrystals were typically 4 nm in diameter with a fairly narrow size distribution. This stems from the good lattice match between two CdSe and three Au spacings (−0.6% mismatch); the crystals are subjected to increasing mismatch strain as they grow, eventually resulting in termination of growth.[9] Measurement of the band gaps of these QDs by normal optical absorption is complicated by the very small amounts of material, resulting in a very low absorption, and, more importantly, by the masking effect of the slightly transparent, highly reflecting Au substrate. For these reasons, we have considered other ways to optoelectronically characterize our samples that would permit the study of the expected increase in band gap.

The two most successful methods were current−voltage spectroscopy using an atomic force microscope with a metallized tip[10] and photocurrent spectroscopy using the sample as a photoelectrode in a liquid junction.[11] Our results using the latter technique comprise the subject of the present paper. We show that an approximate measure of the QD band gap can be made using this technique, even for very small amounts of material, equivalent to a 2.5 nm thick film (less than a monolayer of QDs). Size distribution and sub-band-gap response often result in a somewhat lower effective band gap value than expected for the average QD size based on transmission electron microscopy (TEM) and X-ray diffraction (XRD) measurements. We explain major changes in photocurrent internal quantum efficiency with increased amount of CdSe deposited in terms of different recombination mechanisms. Sub-band-gap photocurrent generation from intra-band-gap states is shown, and supra-band-gap changes in photocurrent due to charge transfer from excited states in the quantum dots are postulated.

Experimental Section

The CdSe nanocrystals were epitaxially grown on (111) textured gold and evaporated on mica substrates, by electrochemical deposition. A two-electrode electrochemical cell was used to carry out the electrochemical deposition with the gold film substrate as the cathode and a graphite rod as the anode in a solution made of $Cd(ClO_4)_2 \cdot H_2O$ or $CdCl_2$ and elemental Se in hot DMSO. The plating was carried out in the constant current (galvanostatic) mode at a given current density, temperature, and time.[8] The amount of CdSe deposited can be calculated from the plating charge (the product of current and time), the CdSe density, and Faraday's law. On the basis of a 2-electron transfer and assuming 100% current efficiency, a homogeneous deposit of 1.7 nm thickness would be formed after 10 s plating at a current density of 0.1 mA/cm^2. We use here the term "nominal thickness" to refer to the thickness which would be obtained with a homogeneous deposit, although our deposits are not homogeneous but are comprised of nanocrystals. Therefore, a deposition time of 30 s would give a nominal thickness of 5 nm.

A Phillips EM-400T microscope operating at 120 kV was used to carry out transmission electron microscopy (TEM) measurements. For TEM characterization, samples were prepared by carefully floating the gold films in a 20% aqueous HF solution, which removed them from the mica substrates, and lifting onto TEM grids. The floating is carried out such that the gold surface with the nanocrystals is never in contact with the HF solution.

X-ray diffraction (XRD) was carried out by lifting the gold films onto an Au sheet that was polished with micropolish alumina (Buehler Ltd.) then placing in a Rigaku RU-200B

* Corresponding author. Fax: 972-8-9344138. E-mail: cphodes@weizmann.weizmann.ac.il.

10.1021/jp983368f CCC: $18.00
Published on Web 05/18/1999

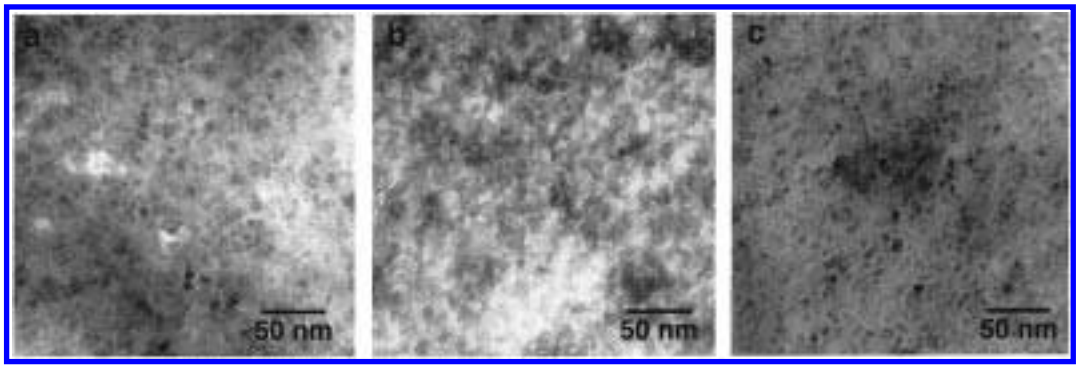

Figure 1. Conventional TEM bright-field images of CdSe nanocrystalline films with nominal thicknesses of 5 nm, corresponding to a full monolayer (a), and 15 nm, a little more than two layers (b), electrodeposited on Au from a $Cd(ClO_4)_2$ solution; c) 15 nm film electrodeposited using $CdCl_2$. Note the smaller size compared with (b). The first QD layer (as in a) is subjected to an epitaxial size-limiting mechanism that results in a smaller size. Subsequent layers (as in b and c) are not in direct contact with the Au substrate and the epitaxy is lost, resulting in an increase of the nanocrystalline size with increasing thickness.

Rotaflex diffractometer operating in the θ-2θ Bragg configuration using Cu Kα radiation. The scan rate was 0.025°/min with a sampling interval of 0.004°. The voltage was set to 45 kV with a 150 mA flux.

Photoelectrochemical measurements were carried out in an electrolyte of aqueous sodium selenosulfate (0.2 M Se and 0.4 M Na_2SO_3) in a two-electrode photoelectrochemical cell, with a Pt counter electrode. A CARY model 17D spectrophotometer with a 600 W tungsten−halogen lamp operating at 80 V (instead of the full rated 120 V) was used as the light source/double monochromator. The sample electrode was connected via a current-to-voltage transimpedance amplifier to a lock-in amplifier, and from there to a recorder. The readings were corrected for the lamp and monochromator response using a calibrated Si diode.

Electrolyte electrotransmission (EET) was performed in the same electrolyte with a modulating sine wave of 0.5 V peak-to-peak.

Results and Discussion

Crystal Size and Band Gap. Figure 1 shows TEM micrographs of CdSe deposited on Au, using $Cd(ClO_4)_2$, for various deposition times. Figure 1a shows a 30 s deposit (nominal thickness is ca. 5 nm). The average crystal lateral dimension is 4−5 nm, as was previously described for similar films.[8,10] It is important to emphasize that the CdSe grows in the form of islands rather than as a coherent layer and that once the first nanocrystalline layer had been completed, subsequent layers of CdSe grow nonepitaxially on top of the CdSe, and crystallite size increases by ca. 2−3 times within a few nanocrystalline layers.[8,12]

A 90 s deposit (ca. 15 nm nominal thickness) is shown in Figure 1b. The size distribution in this case is much wider (both because of the loss of epitaxy, and therefore the strain mechanism which limits crystal size,[9] as well as the underlying layer of smaller crystals) with a typical size of 10 nm. Assuming that the second layer of crystals grows without perturbing the size of the crystallites in the first layer, this deposit represents, to a good approximation, two crystal layers: the first of ca. 5 nm, and the top one of ca. 10 nm. We rule out the possibility that the 15 nm layer is composed of only one layer of crystals, 15 nm in height (as might be inferred from the XRD measurements below). If this were the case, the first epitaxial layer would have to rotate on the Au in order to cause the observed loss of epitaxy of the second layer, an unlikely event. In the case of 30 nm nominal thickness (not shown), even larger crystals, typically between 10 and 15 nm, are seen. It becomes more difficult to quantify the (average) number of crystal layers for these thicker films; however, one can reasonably assume ca. 3 layers.

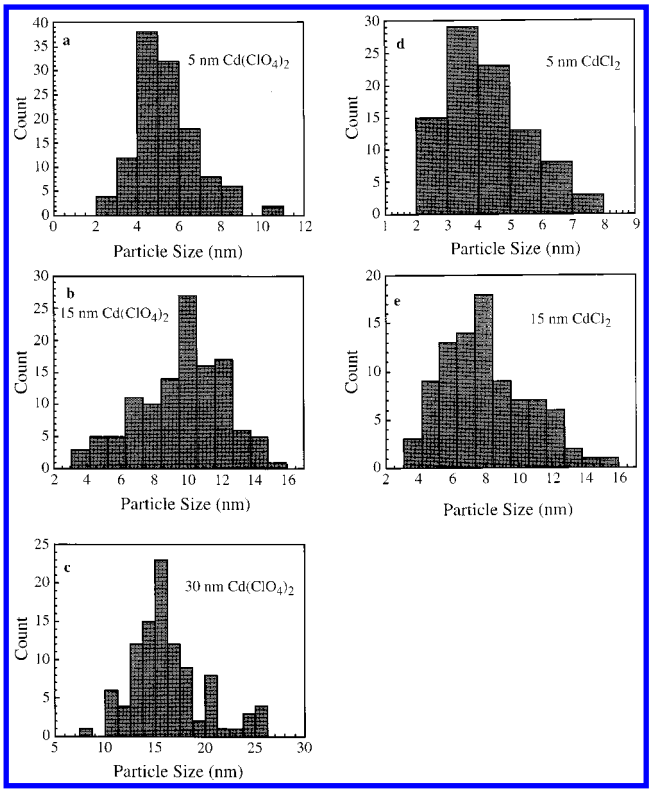

Figure 2. Size distributions for 5, 15, and 30 nm films electrodeposited from $Cd(ClO_4)_2$ solution (a−c) and for 5 (d) and 15 (e) nm films electrodeposited using $CdCl_2$.

The anion of the Cd^{2+} salt used in the electrodeposition is important in determining the crystal size, i.e., the use of chloride results in smaller crystals than does perchlorate. Figure 1c shows a micrograph of a 15 nm deposit obtained under conditions similar to those in Figure 1b, but using $CdCl_2$ instead of $Cd(ClO_4)_2$. In contrast to the respective perchlorate deposition, it is comprised of smaller crystals ca. 8 nm. The 5 nm deposit (not shown) consists mostly of 3−4 nm crystals, slightly smaller than for the 5 nm perchlorate film. This difference between the two anions has been reported previously for much thicker films.[13] It is believed to be due to surface capping by adsorbed chloride ions, blocking the growth of the nanocrystals.[14] Nanocrystallite size distributions for all of these films are shown in Figure 2. It should be kept in mind that these distributions are based on the crystals visible in the TEM micrographs. For

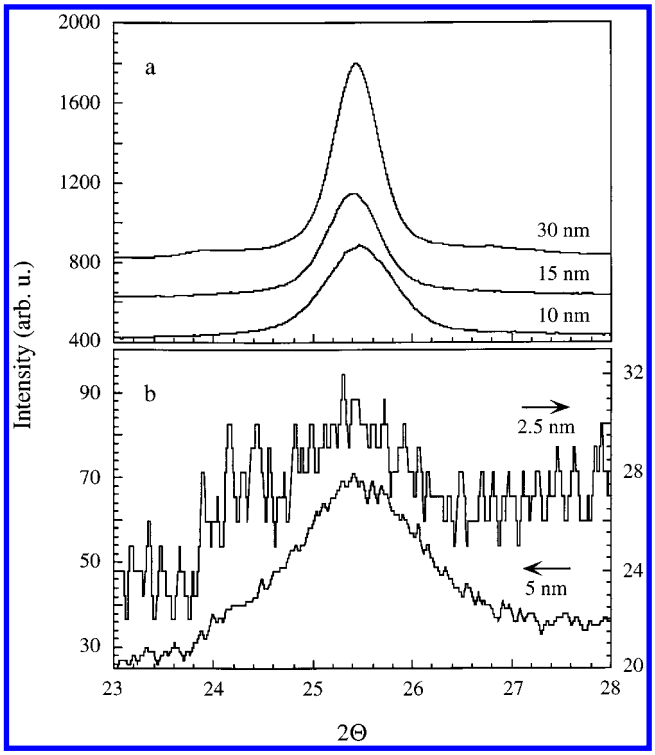

Figure 3. X-ray diffraction spectra of CdSe nanocrystalline films electrodeposited on Au. (a) Thicker films: 30, 15, and 10 nm, as indicated in the figure. (b) Thinner films: 2.5 and 5 nm. The intensity of the 2.5 nm film is shown on the right.

TABLE 1: XRD (Height) and TEM (Lateral) Dimensions for Various $Cd(ClO_4)_2$-Deposited Film Thicknesses

	nominal thickness (nm)				
	2.5	5	10	15	30
crystal size (nm)					
XRD	5	6	12	15	19
TEM		4−5		10	15

the thicker films, this means that much or all of the underlying layer(s) of crystals, which are hidden by the overlying layer, will not be included in the histograms.

The average crystal height can be calculated from the XRD data, using the Debye−Scherrer formula and peak widths.[9] This is shown in Figure 3 for films deposited using $Cd(ClO_4)_2$. Only one peak is shown since the nanocrystals grow epitaxially on the Au surface with a strong preferential orientation, and no other peaks are observed in the spectra. The spectrum of the 2.5 nm film is noisy because of the very small amount of CdSe present on the Au surface. Yet, one can still estimate the height as ca. 5 nm, similar to the lateral dimension measured by TEM. The height of the 5 nm film is found to be ca. 6 nm, somewhat larger than the respective lateral dimension. Nonetheless, since the intensity in XRD is proportional to the square of the number of atoms in the crystal,[15] the resulting spectrum would be dominated by the larger crystals present in the size distribution of our films. Also, as a certain error may be expected when using the Debye−Scherrer formula with such small structures, this height calculation may be considered as an estimate only. The heights of the 10, 15, and 30 nm films are found to be 12, 15, and 19 nm, respectively. These values are close to the lateral dimensions of the upper layers as measured by TEM. The combined crystal dimensions measured from the TEM and XRD are summarized in Table 1.

Figure 4 shows photoelectrochemical spectra of CdSe nanocrystalline films (deposited from a perchlorate solution) as a

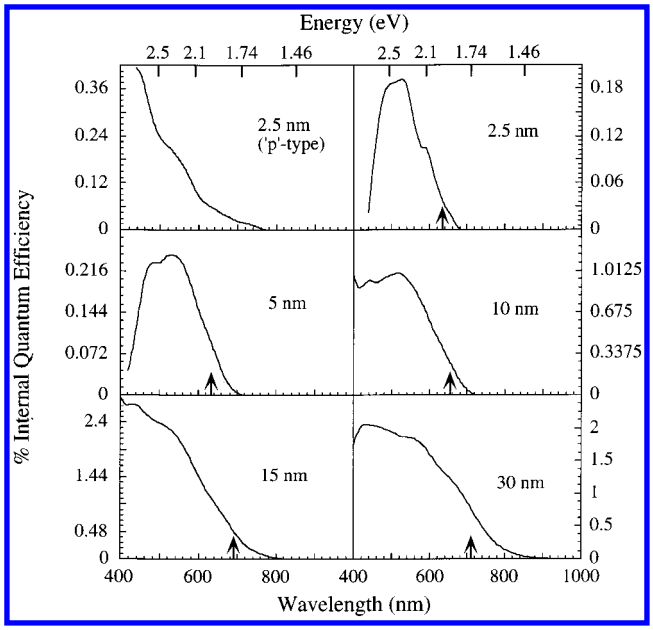

Figure 4. PEC photocurrent spectra of various nominal thicknesses (given in the figure) of CdSe QDs electrodeposited on gold. Here, 2.5 nm is equivalent to half a monolayer of QDs, 5 nm is a full monolayer, 15 nm is a little more than two layers, and 30 nm is at least three. The p-type spectrum shown in the top left was observed with a sample which behaved as p-type (in contrast to the usual n-type behavior). The quantum efficiency was corrected for thickness differences. Arrows indicate the estimated band gap value. Energy (in eV) is given in the top scale.

function of nominal film thickness. To compare the relative response of the different thicknesses, the response of all the samples has been normalized to that of the 30 nm one, assuming that the absorption is a linear function of the thickness (a reasonable assumption for these thicknesses). For example, the measured response of the 15 nm film has been multiplied by two, that of the 10 nm film has been multiplied by three and so on. The result of multiplying the actual measured response of the 10 nm film by the ratio of the thicknesses (three) yields a peak response of the 30 nm sample that is twice that of the 10 nm one. The real difference in peak response before normalization is, therefore, six times. In this paper, we use the term "internal quantum efficiency". This term usually refers to the ratio between electrons out (as photocurrent) and photons absorbed, in contrast to external quantum efficiency, which is the ratio between electrons out and incident photons. It should be kept in mind that, in our case, the real internal quantum efficiency will be much higher than the values given below, since the absorption, even by the 30 nm sample, is low over the whole measured spectral range. While we could not measure this absorption directly on the Au substrates, from other experiments we estimate an absorption of $\approx 10\%$ in the strongly absorbing region for the 30 nm film. Since knowledge of the real quantum efficiency is not essential for the present purpose, the terminology used here is reasonable.

First we consider the values of the band gap (E_g) estimated from these spectra. For the 2.5 nm (ca. half a monolayer of nanocrystals) and 5 nm films (ca. a full monolayer), the cutoff values are similar and the band gap can be estimated, by extrapolating the square of the photoresponse to zero, as ca. 1.95 eV. The 5 nm film has a slight tail extending to lower energies, which could be due to a small fraction of larger crystals. The shoulder in the spectrum of the 2.5 nm film, which occurs frequently in films of this thickness, could be explained by the existence of two predominant crystal sizes, one corre-

sponding to 1.95 eV (ca. 6 nm) and the other to ca. 2.2 eV (< 4 nm). A band gap distribution of similarly electrodeposited isolated CdSe QDs on Au using conductance spectroscopy has shown a predominant band gap value of about 2.2 eV with values down to 1.9 eV.[10] Another possibility is the existence of two separate transitions, with the 2.2 eV transition involving a higher (quantized) energy level.

The 10 nm film (estimated ca. one and a half layers of nanocrystals; less than two since the crystals in the second layer are already somewhat larger than those in the first layer) exhibits a small red shift in E_g to an estimated average value of ca. 1.9 eV. The 15 nm film (≥ 2 layers of nanocrystals) has an average band gap of ca. 1.8 eV and a tail extending to 800 nm (1.55 eV), clearly a sub-E_g component, since the bulk band gap of CdSe is 1.74 eV. This sub-E_g response is even more pronounced in the 30 nm film (at least 3 nanocrystal layers, containing some crystals which are no longer size-quantized (larger than 12 nm) and should have a band gap of 1.74 eV); it extends considerably beyond the bulk band gap value. Sub-E_g response has been observed previously in semiconductor photoelectrodes, and attributed to absorption in intra-band-gap states.[16−18]

The crystal sizes measured by TEM and XRD can be correlated with the expected values of the band gap using other studies. From the experimental results of Murray et al.,[19] the band gap values should be ca. 2.1 eV for the 2.5 and 5 nm films, ca. 1.8 eV for the 15 nm film, and 1.74 eV (bulk value) for the 30 nm film. While the value of 1.8 eV for the 15 nm film agrees well with the one measured here (as can be expected, since in that size range, the band gap does not vary much with crystal size), the 2.1 eV value expected for the thinnest films is considerably greater than the 1.95 eV measured.

There are several possible explanations for this apparent inconsistency. Since there is a certain distribution of crystal sizes, as indicated by our XRD and TEM results, and therefore of band gaps in the films, it is possible that the current onset is dominated by the larger crystals in the distribution which would result in a red shift in the current onset value. This would be particularly pronounced if the photoresponse increased with crystal size. The predominant band gap value of about 2.2 eV with values down to 1.9 eV measured on similar samples (equivalent to a thickness of 0.85 nm[10]) suggests that this explanation is the most likely one.

Another possibility is that the CdSe is not fully quantized in the direction of the substrate, i.e., there is little, if any, barrier between the CdSe and the gold. The occurrence of Coulomb charging in this system, however, implies that such a barrier exists.[20,10]

A third explanation is based on the sub-E_g signals seen in the thicker films. In this context, it is interesting to note that the more quantized films do not show a pronounced sub-E_g response, particularly since the high surface-to-volume ratio of the crystals in these films might suggest such a response. It may be that a high density of surface states may cause a sharp increase in the current that would mask the real band gap response. The existence of such a sub-E_g component would then result in a situation where the actual band gap is higher than the one estimated from the photoresponse spectrum.

Photocurrent Efficiency and Film Thickness. While the estimation of the band gap was the initial objective of this study, the spectra show other intriguing characteristics. One of these is the relative photocurrent at the peak of the response for the different layer thicknesses. For such thin films, the absolute photocurrent is expected to increase approximately proportional to the film thickness (i.e., to the light absorption). Considering first the nanocrystalline films deposited from perchlorate solutions (Figure 4), this is observed between the 2.5 and 5 nm films, and between the 15 and 30 nm films. The 10 nm film, on the other hand, gives an order of magnitude higher absolute photocurrent than the 5 nm film (5 times the internal photocurrent efficiency). The difference between the 10 and 15 nm films is also greater than expected based on thickness alone, although less than the dramatic change between the 5 and 10 nm films (ca. 2.5 times the internal photocurrent efficiency).

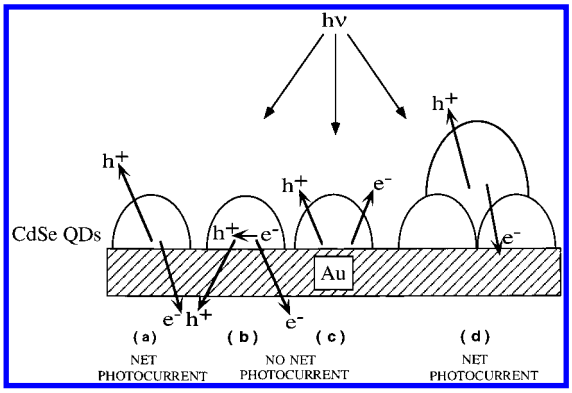

Figure 5. Schematic diagram of photogenerated charge transfer and loss pathways in PEC cells (see text).

To understand this behavior, we must first consider the mechanism of photocurrent generation and loss in a PEC system. Figure 5 shows a schematic diagram of a single CdSe nanocrystal on the gold substrate (a, b, and c) and of two layers of crystals (d). To measure photocurrent, one charge carrier must be transferred to the electrolyte and the counter charge carrier to the Au (Figure 5a shows the situation for an "n-type" response; the direction would be reversed for a "p-type" response). Figures 5b and c represent electron−hole recombination at the Au substrate or in the QD itself and through the electrolyte, respectively. In both cases no photocurrent will be generated. It is not surprising that the collection efficiency for a single layer or less is very low since the electron−hole pair is generated close to the Au surface. Therefore, recombination, either by energy transfer to the gold (nonradiative electron−hole recombination in the QD) or by injection of the photogenerated electron and hole into the gold, is expected to be an easier path than transfer of one of the charges to the electrolyte.

When charge generation occurs in the second layer of crystals (Figure 5d), recombination will be reduced, whether it occurs by charge transfer or by energy transfer. In the former case, for recombination through the substrate to occur both charges have to pass through an additional barrier between the two crystallites. In this case there is a better chance that one of the charges generated in the second layer would be transferred to the electrolyte. Hence, the probability of recombination through the substrate decreases with the number of crystal boundaries that both charges must cross. In the latter (energy transfer), the increased distance necessary for energy transfer will lower the probability of recombination due to the Au.

Recombination by Charge Transfer. The fact that the major change in collection efficiency occurs between the first and the second crystal layers suggests that the barrier for charge transfer, due to grain boundaries between individual nanocrystals, is sufficiently high to allow one of the charges to react with the electrolyte in preference to transfer from one crystal to another. This is not surprising, as a similar assumption of an intercrystalline barrier to charge transfer is necessary to explain the observed spectral shifts in aggregated nanocrystalline films.[3] These shifts are characteristic of size quantization in isolated

nanocrystals of the same size, indicating the existence of an intercrystal barrier to charge transfer.

The above results present an interesting, counter-intuitive conclusion: In the system described here, grain boundaries *improve* the photocurrent collection efficiency rather than decrease it as is usually the case with bulk and other nanocrystalline[3,4,21] semiconductor photovoltaic cells. The electrolyte makes contact with each individual nanocrystal in the somewhat porous film; this means that the photogenerated charges are created essentially at the crystal surface and one of them (usually the hole) can be readily transferred to the electrolyte.[3] The other charge (usually the electron) has to pass through crystal boundaries, the number of which depends on film thickness and crystal size, to reach the substrate. As noted above, holes are assumed to be rapidly removed by the electrolyte; since there are few, if any, nonphotogenerated holes in the (intrinsic) CdSe, there is little opportunity for recombination except with film thicknesses much greater than 100 nm (i.e., many more crystal boundaries). Recent studies of nanocrystalline CdSe films have shown that the preferential transfer of holes (electrons) to the electrolyte is due to preferential trapping of holes (electrons) at the QD surfaces.[7] In the present case, the trap sites clearly have a low enough recombination cross-section and/or the kinetics of charge transfer to the electrolyte are sufficiently fast so that this does not cause a major loss in electron (hole) transfer to the electrode for films which are not too thick.

Recombination by Energy Transfer. An excited e/h pair can recombine nonradiatively by energy transfer (ET), whereby the energy of the excited state is transferred through space by a dipole−dipole interaction to a nearby (< 10 nm) acceptor.[22] This mechanism can explain the rapid quenching of photoluminescence from excited molecules at metal surfaces. While both ET and the charge transfer mechanism discussed above involve e/h recombination, in the former the electron and hole recombine in the same QD rather than being transferred to the Au substrate. In the ET mechanism, an important factor is the distance of the donor (the excited QD) from the acceptor (the Au). The second layer of QDs is farther away (ca. 4 nm) from the Au, and the ET, resulting in loss of photocurrent, will be less. For the third layer (> 10 nm from the Au), ET should no longer be possible to any appreciable degree. It is difficult to distinguish between the two mechanisms in our results.

Counterion Effect. The photocurrent spectra of the CdSe films deposited from a chloride solution are shown in Figure 6. For all thicknesses, the estimated band gaps are considerably lower than expected on the basis of the measured crystal size. In this respect, the explanations suggested above for this phenomenon can be employed here, too. Moreover, the same trend in the relative photocurrent efficiency seen in the perchlorate samples is also observed here: There is a very large difference between the 2.5 and 5 nm films (ca. 3 orders of magnitude), a large difference between the 5 and 10 nm films (ca. 30 times), a moderate difference between the 10 and 15 nm films (three times) and no difference between the 15 and 30 nm films. Because of the smaller crystal size in the chloride case, a monolayer of crystals would be nominally equivalent to 3−4 nm thickness. The 2.5 nm film is certainly less than a monolayer of crystals, and, in view of the very small crystal size, almost all of the photogenerated charges would recombine at the substrate. While the 5 nm film is probably not much more than a monolayer of crystals, there may be a small fraction of crystals sitting on other crystals rather than directly on the gold. In view of the very large differences in quantum efficiency between the various thin films, even a very small percentage

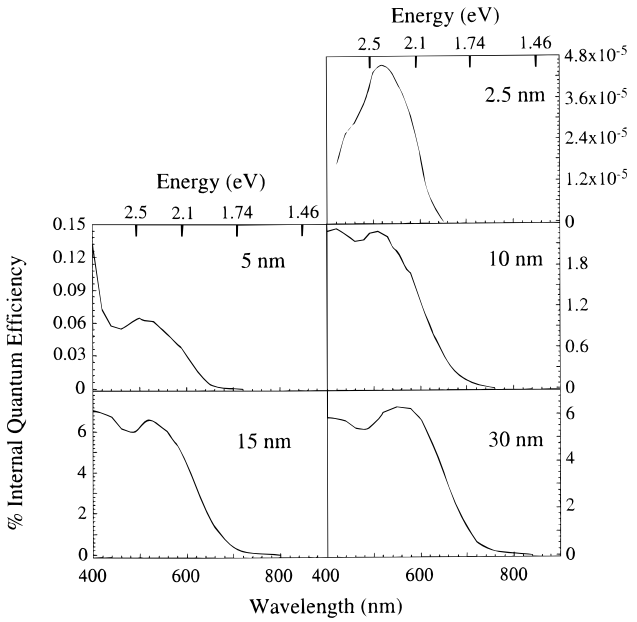

Figure 6. PEC photocurrent spectra of various nominal thicknesses (given in the figure) of CdSe QDs electrodeposited from a $CdCl_2$ solution. The thicknesses are similar to those in Figure 4. In all cases the quantum efficiency was corrected for thickness differences. Top scale shows the energy (in eV).

of crystals not directly in contact with the gold would make a large difference in photocurrent. Though it is difficult to say whether there is a large difference between the photocurrent generation in the second and third layers of crystals, there is clearly a very large difference between the first and the second layers. Thus, the smaller chloride-deposited crystals behave in this respect like the larger perchlorate-deposited ones, only to a greater extent.

The thicker (≥ 10 nm) chloride-deposited CdSe films exhibit a higher quantum efficiency than the corresponding perchlorate-deposited ones. The same trend was noticed in much thicker (> 100 nm) films of CdSe nanocrystals deposited in a similar manner.[13] Possible explanations for this difference are the different surface properties of the two films or bulk recombination in the larger perchlorate-deposited crystals.

Hot Hole Transfer. The peak between 2.4 and 2.5 eV in the spectra of the thin films (2.5 and 5 nm perchlorate-deposited and 2.5 nm chloride-deposited) cannot be explained by either surface recombination (a common explanation for such a feature in the spectra of bulk semiconductors) or charge generation far from the substrate which could result in greater recombination losses at grain boundaries.[3] We suggest that the phenomenon may reflect photocurrent arising from transition to higher energy levels in these (quantized, therefore having discrete levels) nanocrystals. The decrease in response occurs at an energy of ca. 0.5 eV above the first excited state. The transition which best fits this energy is from the spin−orbit split-off valence level ($1S_{1/2}$) to the first ($1S_e$) conduction level ($E_g + 0.45$ eV).

Electrolyte electrotransmission (EET) spectroscopy shows this transition quite clearly, as shown in Figure 7. The major feature, at ca. 640 nm (1.94 eV), is the "band gap" transition while the smaller one at ca. 510 nm (2.43 eV) is attributed to the transition from the spin−orbit split-off valence level to the first conduction level. The energy difference of ca. 0.49 eV between the two features is similar to that between the (almost degenerate) light and heavy hole bands and the spin−orbit split-off band in bulk CdSe. Since the hole effective masses in the light hole band and split-off band are very similar in CdSe, we might expect

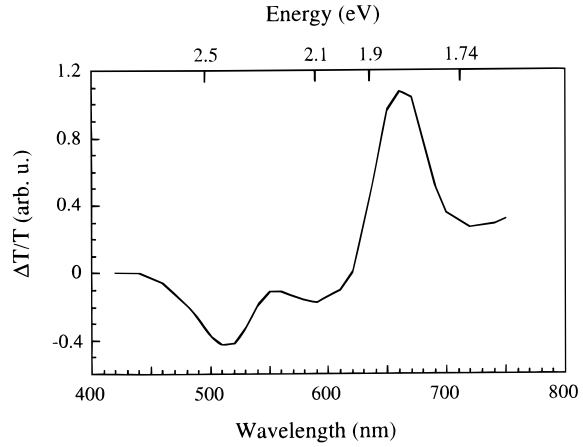

Figure 7. EET spectrum of 10 nm (nominal; equivalent to 1.5 − <2 crystal layers) CdSe QD film electrodeposited from a $Cd(ClO_4)_2$ solution. Top scale shows the energy (in eV).

both bands to behave similarly upon size quantization, ignoring complications such as mixing of levels. A value of 1.94 eV for E_g is estimated on the basis of the symmetry of the spectrum in Figure 6. Since the film comprises (almost) two layers of crystals, the first (adjacent to the Au) with a size of ca. 4−5 nm and the second with somewhat larger QDs, the spectrum reflects a moderate size distribution which would complicate curve-fitting. From the (room temperature) results of Murray et al.[19] this translates to an average size of 6 nm, which is somewhat larger than the first nanocrystal layer and smaller than crystals in a layer ca. 2−3 times that thickness.

On the basis of these observations, we speculate that the higher energy feature is connected with a decrease in the hole transfer to the electrolyte and to the generation of higher energy (hot) holes. The probability of hot carrier effects in our system is increased by two effects. The very small size of the nanocrystals means that charges are generated essentially at the semiconductor/electrolyte interface (charge delocalization over all or most of the crystal) and do not have to travel an appreciable distance to reach this interface. The second effect is the expected longer thermalization times in widely spaced, quantized levels.[23]

For the energy transfer mechanism, the energy transfer increases with increasing recombination energy, resulting in a decrease in photocurrent. On the basis of the charge transfer mechanism, hot holes should be more readily transferred to the Au, resulting in increased recombination at the substrate. This is because the competitive hole transfer rate to the electrolyte will be less for a hot hole than for a thermalized one (the overlap between the levels of the oxidized electrolyte and hot hole level will be less than for the thermalized hole level). When more than one crystal boundary is involved (two or more layers of crystals), the hot hole would thermalize by the time it passed through the first crystal boundary, hence is more likely to be trapped and transferred to the electrolyte. This would explain the fact that no decrease in response is seen in films with two or more crystal layers.

Further support for the hot hole hypothesis is given by the PEC spectrum of a 2.5 nm film (Figure 4) which shows a p-type behavior (the as-prepared films usually show an n-type behavior; however, they occasionally show p-type behavior for reasons unknown at present). The striking feature in this spectrum is the *increase* in photocurrent at the same photon energy where the n-type samples exhibit a *decrease* in photocurrent. This observation is consistent with our previous explanation: Hot holes are generated at ca. 2.5 eV and more readily recombine at the Au surface with the large excess of free electrons in the metal. Since, in this case, this is the direction of charge flow required to produce photocurrent (in contrast to the n-type samples), the result is an increase in photocurrent due to the generation of hot holes. This explanation is only valid for the charge transfer mechanism of recombination; the energy transfer mechanism is not dependent on the direction of charge transfer.

Conclusions

We have measured the increase in the band gap of electrodeposited CdSe quantum dots using liquid-junction photocurrent spectroscopy. The photoresponse of the 2.5 and 5 nm films of QDs (4−5 nm in size) is very low because of a high recombination, either by energy or charge transfer to the Au surface, but increases considerably for the second and subsequent layers. This marked difference is explained in the charge transfer mechanism by the role of grain boundaries in enhancing collection efficiency in these films and in the energy transfer mechanism by the greater separation between the excited nanocrystal and the Au. A prominent sub-band gap response, extending considerably beyond the bulk band gap value, was observed for the thicker films. Hot hole transfer is suggested to explain the decrease in the photocurrent at short wavelengths, which occurs for the very thin films on Au.

Acknowledgment. We thank Irit Ruach-Nir for her assistance in TEM characterization. This research was supported by the United States−Israel Binational Science Foundation, Jerusalem, Israel, Grant no. 94-00103 (G.H.) and by the U.S. Office of Naval Research, Grant no. N00014-1-1151 (G.H. and I.R.).

References and Notes

(1) Yoffe, A. D. *Adv. Phys.* **1993**, *42*, 173.
(2) O'Regan, B.; Grätzel, M. *Nature* **1991**, *353*, 737.
(3) Hodes, G.; Howell, I. D. J.; Peter, L. M. *J. Electrochem. Soc.* **1992**, *139*, 3136.
(4) Hagfeldt, A.; Bjorksten, U.; Lindquist, S.-E. *Sol. Energy Mater. Sol. Cells* **1992**, *27*, 293.
(5) Liu, D.; Kamat, P. V. *J. Phys. Chem.* **1993**, *97*, 10769.
(6) Hodes, G.; Howell, I. D. J.; Peter, L. *Photochemical and Photoelectrochemical Conversion and Storage of Solar Energy*; Tian, Z. W., Cao, Y., Eds.; International Academic Publishers: Beijing, 1993; p 331.
(7) Kronik, L.; Ashkenasy, N.; Leibovitch, M.; Fefer, E.; Shapira, Y.; Gorer, S.; Hodes, G. *J. Electrochem. Soc.* **1998**, *145*, 1748.
(8) Golan, Y.; Margulis, L.; Rubinstein, I.; Hodes, G. *Langmuir* **1992**, *8*, 749.
(9) Golan, Y.; Hodes, G.; Rubinstein, I. *J. Phys. Chem.* **1996**, *100*, 2220.
(10) Alperson, B.; Cohen, S.; Rubinstein, I.; Hodes, G. *Phys. Rev. B* **1995**, *52*, R17 017.
(11) Alperson, B.; Cohen, S.; Golan, Y.; Rubinstein, I.; Hodes, G. NATO ASI Series 3; E. Pelizzetti, Ed.; 1996; p 579.
(12) Golan, Y.; Alperson, B.; Hutchison, J. L.; Hodes, G.; Rubinstein, I. *Adv. Mater.* **1997**, *9*, 236.
(13) Hodes, G.; Engelhard, T.; Albu-Yaron, A.; Pettford-Long, A. *Mater. Res. Soc. Symp. Proc.* **1990**, *164*, 81.
(14) Mastai, Y.; Gal, D.; Hodes, G., manuscript in preparation.
(15) Warren, B. E. *X-ray Diffraction*, 1st ed.; Dover Publications, Inc.: New York, 1990.
(16) Iranzo Marin, F.; Hamstra, M. A.; Vanmaekelbergh, D. *J. Electrochem. Soc.* **1996**, *143*, 1137.
(17) Chazalviel, J.-N. *J. Electrochem. Soc.* **1980**, *127*, 1822.
(18) Laser, D.; Gottesfeld, S. *J. Electrochem. Soc.* **1979**, *126*, 475.
(19) Murray, C. B.; Norris, D. J.; Bawendi, M. G. *J. Am. Chem. Soc.* **1993**, *115*, 8706.
(20) Meirav, U.; Foxman, E. B. *Semicond. Sci. Technol.* **1995**, *10*, 255.
(21) Bedja, I.; Hotchandani, S.; Kamat, P. V. *J. Phys. Chem.* **1994**, *98*, 4133.
(22) Waldeck, D. H.; Alivisatos, A. P.; Harris, C. B. *Surf. Sci.* **1985**, *158*, 103.
(23) Boudreaux, D. S.; Williams, F.; Nozik, A. J. *J. Appl. Phys.* **1980**, *51*, 2158.